

室内可见光通信亮度可控混合多层 OFDM 调制方法

任嘉伟, 汪涛, 徐志坚, 曲晶*

中国人民解放军战略支援部队信息工程大学信息工程学院, 河南 郑州 450001

摘要 针对室内可见光通信的照明一体需求,为实现高效数据通信和调光控制相结合,在多层非对称裁剪光正交频分复用(LACO-OFDM)信号分时正负叠加调光方法的基础上,通过在LACO-OFDM信号上叠加一个经过设计的周期信号来产生叠加的LACO-OFDM(SLACO-OFDM)信号,可以在不引入额外干扰的情况下,降低多层信号的峰均功率比。再利用正负SLACO-OFDM信号按比例结合的方式来实现混合调光。分析了通信和调光约束条件下,层间功率比例因子和混合比例因子的设置方法。提出的混合SLACO-OFDM具有更小的峰均功率比,充分利用了发光二极管(LED)整个动态范围。仿真结果表明,提出的调制方法相对于传统的多层传输方式可以获得更好的误码率性能,相对于常见调光调制方式可以获得更高的频谱效率。

关键词 光通信; 可见光通信; 调光控制; 峰均功率比; 混合多层调制

中图分类号 TN929.1 文献标志码 A

DOI: 10.3788/CJL230589

1 引言

近年来,个人移动通信、无线互联网业务快速发展,高密度室内通信需求增长旺盛。传统的无线电射频通信受各种限制,难以实现室内高速高密度无线传输。基于发光二极管(LED)的可见光通信方式具备照明一体、低功耗、泛在、宽带、与现有电磁频段不重合等特性,是实现室内高速高密度通信的理想途径^[1]。室内可见光通信系统一般需同时提供通信和照明服务,为了满足室内照明的标准要求,室内可见光通信系统必须具备亮度控制(也称为调光控制)功能^[2]。因此,设计能够进行调光控制的室内可见光信号调制方式势在必行。室内高速可见光通信常使用正交频分复用(OFDM)调制实现高速传输,传统的光OFDM研究主要集中在提高数据传输速率上,不能有效地支持调光控制^[3],导致用户体验不良^[4]。因此,需设计适应照明一体应用的可调光OFDM调制方案。

在OFDM调光设计方面,需兼顾传输效率和调光能力。直流偏压光OFDM(DCO-OFDM)直接通过控制直流偏压水平来控制DCO-OFDM的亮度水平,但可能导致限幅从而破坏信号波形^[5]。与DCO-OFDM相比,非对称裁剪光OFDM(ACO-OFDM)具有更高的光功率效率^[6],被多数调光OFDM方式所使用。非对称裁剪直流偏压光OFDM(ADO-OFDM)^[7-8]是一种混合OFDM形式,在奇数子载波上使用ACO-OFDM,在偶数子载波上使用DCO-

OFDM。另一种称为混合非对称裁剪光OFDM(HACO-OFDM)^[9]的混合OFDM在奇数子载波上使用ACO-OFDM信号,在偶数子载波的虚部上使用脉冲幅度调制离散多音(PAM-DMT)信号。此外,非对称混合光OFDM(AHO-OFDM)^[10]在奇数子载波和偶数子载波上分别使用ACO-OFDM和反向PAM-DMT。上述调制方法的调光控制也是通过改变直流偏置电平获得的,调光范围都较窄,且直接使用ACO-OFDM的传输效率仍较低^[11-12]。重建多层非对称裁剪光OFDM(RLACO-OFDM)^[13]通过正负叠加分层多层非对称裁剪光OFDM(LACO-OFDM)的方式,既实现了调光,又利用了LACO-OFDM的多层传输方式提高了频谱效率^[14],传输性能优于ADO-OFDM、HACO-OFDM和AHO-OFDM。在此基础上,自适应偏压多层光OFDM(ABLO-OFDM)^[15]又通过增加偏移修正进一步提高了频谱效率。但是,LACO-OFDM的多层叠加特性导致峰均功率比较高^[14],在特定的调光等级下会出现误码率(BER)性能变差的问题。

针对可见光通信的照明需求和调光要求,本文首先在LACO-OFDM调制的基础上,提出降低峰均功率比的叠加LACO-OFDM(SLACO-OFDM)调制及其负向调制NSLACO-OFDM,以此为基础信号,提出了一种混合SLACO-OFDM(HSLACO-OFDM)调制方式。通过将SLACO-OFDM和NSLACO-OFDM信号相结合,充分利用了LED整个动态范

收稿日期: 2023-03-06; 修回日期: 2023-04-25; 录用日期: 2023-05-22; 网络首发日期: 2023-07-04

基金项目: 国家自然科学基金(62271505)

通信作者: *jingqu_vlc@163.com

围,且亮度可调。该方案在频谱利用率上比其他常见调光 OFDM 方案高,可以实现通信和调光一体化设计。

2 带调光控制的 HSLACO-OFDM 调制方法

2.1 HSLACO-OFDM 调制信号模型

可见光通信系统一般采用强度调制与直接检测方式,受 LED 发光限制,时域信号必须是正实的,这就要求 OFDM 信号在频域中满足厄米对称性^[16-17]。对于 ACO-OFDM 信号 $x_{ACO} = \{x_1, x_2, \dots, x_N\}$,仅在奇数子载波上调制数据,其对称性可表示为

$$x_n = -x_{n+\frac{N}{2}}, \quad 0 \leq n < \frac{N}{2}. \quad (1)$$

LACO-OFDM 组合了不同层次的 ACO-OFDM 信号。在第 l 层 ($1 \leq l \leq L, L$ 为总的叠加层数)中,只有第 $2^{l-1}(2k+1)$ 层 ($0 < k < N/2^l$)子载波被调制,它们被表示为 $X_{2k+1}^{(l)}$ ($0 \leq k < N/2^l - 1$)。LACO-OFDM 信号在通过 LED 发射时,由于光强度受限,还会产生双向限幅作用,其负向信号将被消减到 0,正向信号超过最大幅度的将被限幅^[18]。在接收端,通过逐层相消的策略,可以一层一层地恢复信号^[19]。

根据 LACO-OFDM 信号的形成原理和各层子载波占用情况可以看出,经过 L 层的信号叠加后,仍会有部分子载波未被使用^[20]。在这些子载波上叠加调整信号,对 LACO-OFDM 各层信号不会产生干扰^[21]。因此,我们可以设计一个使用这些子载波的信号,与原信号叠加后调整 LACO-OFDM 信号的时域幅度。

限幅后的 LACO-OFDM 的一个时域符号可以表示为一个 N 点序列 $Y = \{y_1, y_2, \dots, y_N\}$ 。首先,将该序列分为 $N/2^l$ 组,每组均记为

$$Y_n = \{y_n, y_{n+N/2^l}, \dots, y_{n+iN/2^l}\}, \quad (2)$$

式中: $i = 0, 1, \dots, 2^l - 1; n = 0, 1, \dots, N/2^l - 1$ 。

然后定义周期为 $N/2^l$ 的周期信号 s_n 。 s_n 由以下公式给出:

$$s_n = \max(|Y|) - \max(|Y_n|), \quad (3)$$

式中: $\max(\cdot)$ 表示取序列的最大值。该信号满足 $s_{n+N/2^l} = s_n$ 。

最后,对时域符号 y 进行修正,获得叠加后的 SLACO-OFDM 符号:

$$\tilde{Y} = \{Y_n + s_n\}, \quad n = 0, 1, \dots, N/2^l - 1. \quad (4)$$

对每个符号进行上述混合运算,获得 SLACO-OFDM 信号,记作 Y_{SL} 。

对于 SLACO-OFDM 信号,接收机还可以使用与 LACO-OFDM 信号检测相同的连续干扰消除的方法来逐层检测信号。接收机接收到分层叠加信号后,首先对信号进行快速傅里叶变换(FFT)。 s_n 的 FFT 变换序列 S_i 为

$$S_i = \frac{1}{\sqrt{N}} \sum_{n=0}^{N-1} s_n \exp\left(\frac{-j2\pi ni}{N}\right) =$$

$$\frac{1}{\sqrt{N}} \sum_{n=0}^{N/2^l-1} \left[s_n \exp\left(\frac{-j2\pi ni}{N}\right) \sum_{k=0}^{2^l-1} \exp\left(\frac{-j2\pi ki}{N}\right) \right], \quad (5)$$

式中: $i = 0, 1, \dots, N-1$, 并且

$$\sum_{k=0}^{2^l-1} \exp\left(\frac{-j2\pi ki}{N}\right) = \begin{cases} 2^l, & i = m2^l \\ 0, & \text{otherwise} \end{cases}. \quad (6)$$

然后,式(5)可以重写为

$$S_i = \begin{cases} \frac{2^l}{\sqrt{N}} \sum_{n=0}^{N/2^l-1} s_n \exp\left(\frac{-j2\pi ni}{N}\right), & i = m2^l \\ 0, & \text{otherwise} \end{cases}. \quad (7)$$

根据式(7), s_n 的 N 点 FFT 仅落在未被使用的 $m2^l$ ($m = 0, 1, \dots, N/2^l - 1$)子载波上,不会干扰 LACO-OFDM 的各层有用符号。因此,SLACO-OFDM 信号可以由成熟的 LACO-OFDM 接收结构直接解码。

图 1 给出了一个 $N=16, L=2$ 的 SLACO-OFDM 信号的例子。从图 1 可以看出,LACO-OFDM 信号 Y_n 必为正实,而一个 LACO-OFDM 符号的最大值 $\max(Y)$ 必然也是正实的,当 s_n 与 LACO-OFDM 信号叠加后,所得的信号必然是正实的且每组 Y_n 的最大值必然和 $\max(Y)$ 是相等的,因此叠加后的 SLACO-OFDM 符号的最大值与原 LACO-OFDM 信号的最大值相同,故而 SLACO-OFDM 信号的幅度必然在 LED 的动态范围之内,不会被上限幅。因此,其层间干扰性能与 LACO-OFDM 层间干扰性能^[14]相同。

使用本文所述方法,可以通过叠加一个经过设计

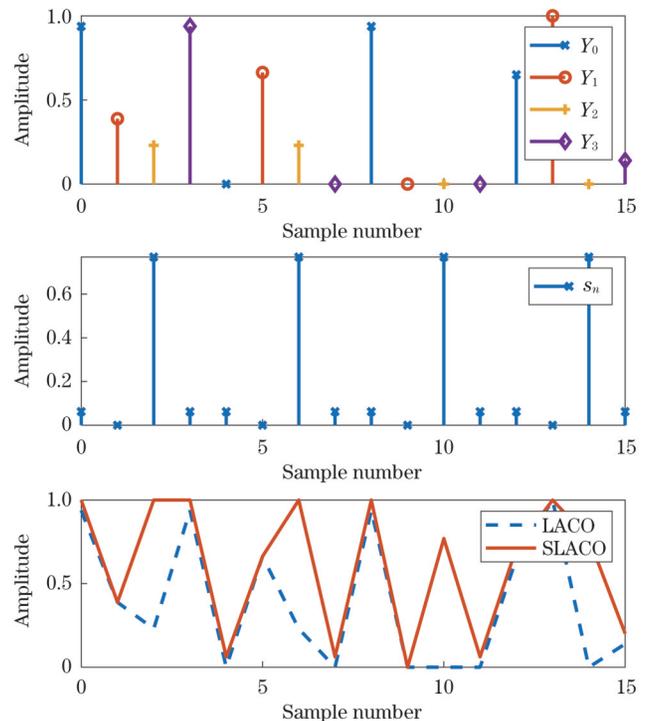


图 1 SLACO-OFDM 信号波形实例 ($N=16, L=2$)

Fig. 1 Example waveforms of SLACO-OFDM ($N=16, L=2$)

的周期信号来产生 SLACO-OFDM 信号。在叠加之后, SLACO-OFDM 信号的峰均功率比将得到改善, 且不引入任何额外干扰。

从式(1)可以看出, ACO-OFDM 的正负部分具有相同的信息, 因此也可以将 ACO-OFDM 信号的正部分去除, 由于对称性, 原信息仍然可以被很好地保留^[22], 从而产生负的 ACO-OFDM (NACO-OFDM) 信号。与 SLACO-OFDM 形成过程类似, NSLACO-

OFDM 使用 NACO-OFDM 信号代替 ACO-OFDM 用于每一层, 记其时域符号 Z , 按照上述方法分组并获得周期信号 s_n 后, NSLACO-OFDM 符号叠加方式为

$$\tilde{Z} = \{Z_n - s_n\}, n = 0, 1, \dots, N/2^L - 1. \quad (8)$$

对每个符号进行上述混合运算, 获得 NSLACO-OFDM 信号, 记作 Z_{SL} 。

2~4 层 SLACO-OFDM/NSLACO-OFDM 信号的波形如图 2 所示。

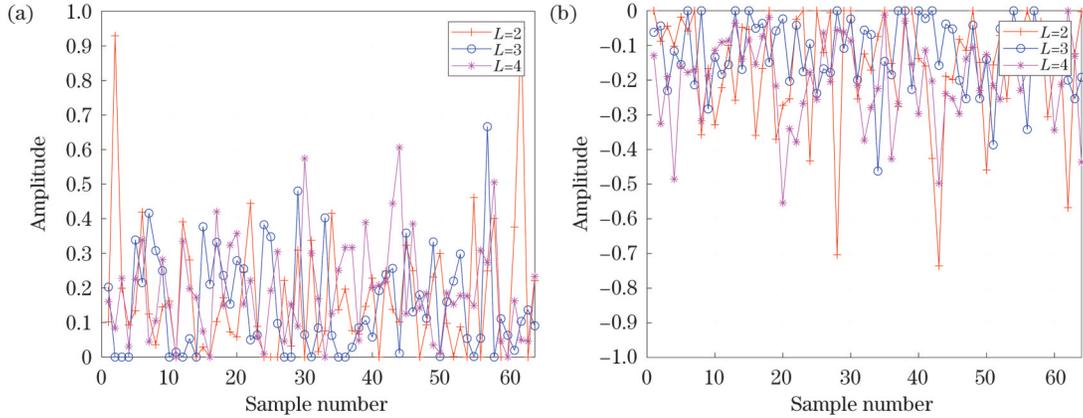


图 2 SLACO-OFDM/NSLACO-OFDM 信号波形。(a)SLACO-OFDM 信号;(b)NSLACO-OFDM 信号

Fig. 2 Waveforms of SLACO-OFDM/NSLACO-OFDM signals. (a) SLACO-OFDM signal; (b) NSLACO-OFDM signal

根据中心极限定理, 第 l 层时域中的 ACO-OFDM 信号服从限幅高斯分布, 可表示为^[23]

$$f_{x_{ACO}^{(l)}}(\omega) = \frac{1}{\sqrt{2\pi} \sigma_l} \exp\left(\frac{-\omega^2}{2\sigma_l^2}\right) u(-\omega) + \frac{1}{2} \delta(\omega), \quad (9)$$

式中: σ_l 表示第 l 层中未限幅信号的均方根; $\delta(\omega)$ 为狄拉克函数; $u(\omega)$ 为单位阶跃函数。

经过限幅后的信号的平均振幅可表示为

$$E(x_{ACO}^{(l)}) = \frac{\sigma_l}{\sqrt{2\pi}}. \quad (10)$$

类似地, NACO-OFDM 信号的概率密度函数 (PDF) 可表示为

$$f_{x_{NACO}^{(l)}}(\omega) = \frac{1}{\sqrt{2\pi} \sigma_l} \exp\left(\frac{-\omega^2}{2\sigma_l^2}\right) u(-\omega) + \frac{1}{2} \delta(\omega), \quad (11)$$

NACO-OFDM 信号的平均振幅也可以表示为

$$E(x_{NACO}^{(l)}) = -\frac{\sigma_l}{\sqrt{2\pi}}. \quad (12)$$

L 层 SLACO-OFDM 信号的 PDF 可以通过每层的 ACO-OFDM 信号和调整信号的 PDF 卷积获得:

$$f_{Y_{SL}}(\omega) = f_{x_{ACO}^{(1)}}(\omega) \otimes f_{x_{ACO}^{(2)}}(\omega) \otimes \dots \otimes f_{x_{ACO}^{(L)}}(\omega) \otimes f_s(\omega), \quad (13)$$

式中: \otimes 为卷积运算符。

从式(11)和式(9)可以看出, NSLACO-OFDM 的 PDF 与 SLACO-OFDM 的 PDF 对称, 后者表示为

$$f_{Z_{SL}}(\omega) = f_{Y_{SL}}(-\omega). \quad (14)$$

图 3 描述了 3 层 SLACO-OFDM/NSLACO-OFDM 和 4 层 SLACO-OFDM/NSLACO-OFDM 的 PDF 图形, 其中 $\sigma_1=0.25$, $\sigma_2=0.25/\sqrt{2}$, $\sigma_3=0.25/2$, $\sigma_4=0.25/2\sqrt{2}$ 。可以注意到 SLACO-OFDM 和 NSLACO-OFDM 的 PDF 是对称的。

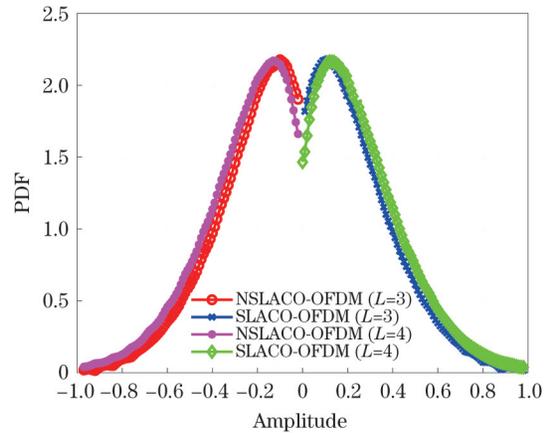


图 3 SLACO-OFDM/NSLACO-OFDM 信号的 PDF

Fig. 3 PDFs of SLACO-OFDM/NSLACO-OFDM signals

调光控制是可见光通信系统适应不同室内照明要求的基本需求, 也是可见光通信系统与其他室内无线通信系统的最大区别。对光信号来说, 可以通过调整平均振幅 (表示为 I_D) 实现调光控制。在有限范围内, LED 的传输特性是近似线性的^[18]。因此, 假设光信号的受限动态范围为 $[I_L, I_H]$, 可以将调光级别定义为

$$\eta = \frac{I_D - I_L}{I_H - I_L} \quad (15)$$

由于 I_D 必须在 $[I_L, I_H]$ 范围内, 调光水平 η 的取值范围为 $[0, 1]$ 。

为确保信号处于 LED 的线性范围内且动态范围得到充分利用, 可以向 L 层 SLACO-OFDM 和 NSLACO-OFDM 信号添加适当的直流偏置, 其大小由下式给出:

$$\begin{cases} I_Y = I_L + Y_{sl} \\ I_Z = I_H + Z_{sl} \end{cases} \quad (16)$$

在 HSLACO-OFDM 方案中, 通过时分复用组合

I_Y 和 I_Z 信号实现调光。设在一个连续 HSLACO-OFDM 信号中, I_Z 的比例为 α , 则 I_Y 占据整个信号的 $(1 - \alpha)$, 在具体实现时, 假设通信信号足够长, 对每个时域符号, 产生一个 $[0, 1]$ 之间的随机数 r , 根据比例因子确定该符号的输出电流为

$$I_o = \begin{cases} I_Z, & r \leq \alpha \\ I_Y, & r > \alpha \end{cases} \quad (17)$$

对每个符号重复上述步骤后获得 HSLACO-OFDM 信号。HSLACO-OFDM 信号的调制原理如图 4 所示。图 4 中 QAM 表示正交幅度调制。

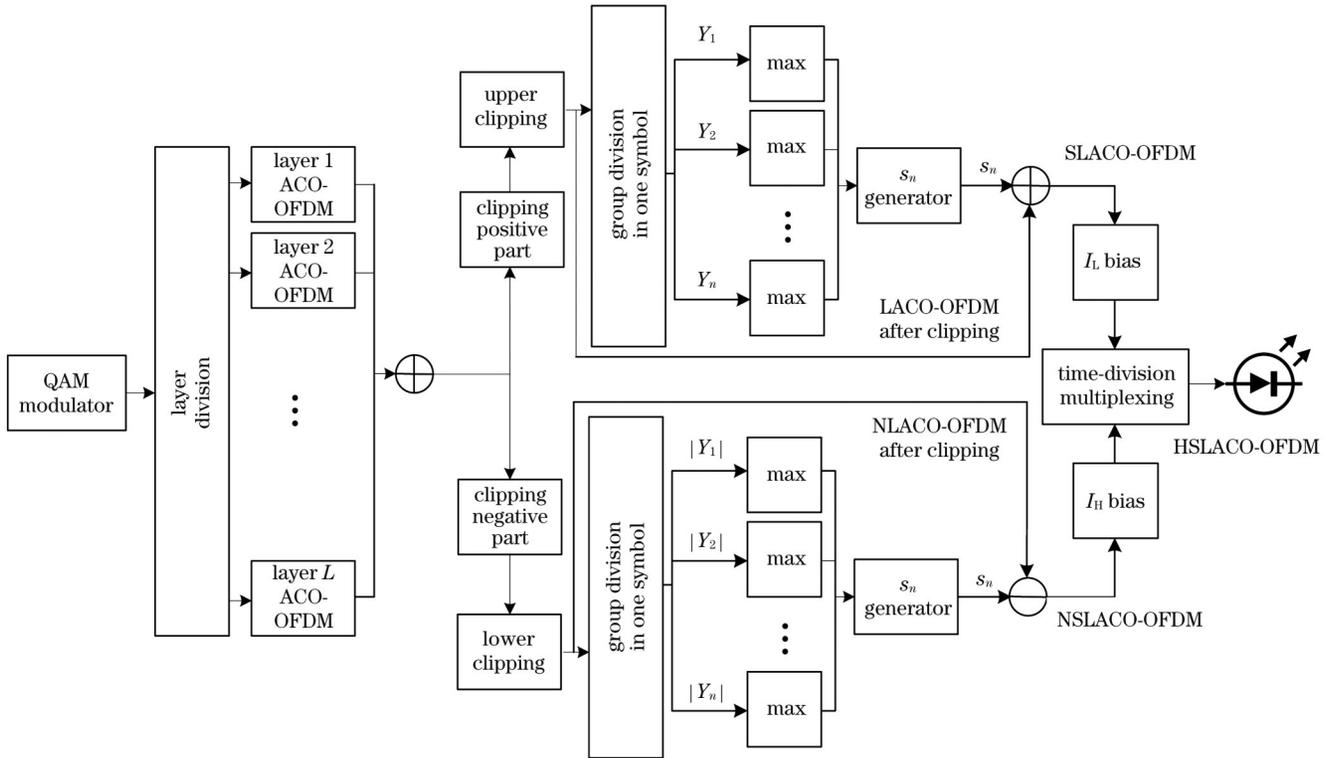


图 4 HSLACO-OFDM 信号调制原理结构图

Fig. 4 Principle structure of HSLACO-OFDM signal modulation

根据式 (10) 和式 (12), HSLACO-OFDM 信号的平均振幅可以近似认为是

$$I_D = (1 - \alpha) \left(I_L + \sum_{l=1}^L \frac{\sigma_l}{\beta_l \sqrt{2\pi}} + \sigma_{s_n} \right) + \alpha \left(I_H - \sum_{l=1}^L \frac{\sigma_l}{\beta_l \sqrt{2\pi}} - \sigma_{s_n} \right), \quad (18)$$

式中: β_l 为 l 层的功率比例因子。

混合传输的 HSLACO-OFDM 信号的波形如图 5 所示, 其中 α 设置为 0.4, 并且子载波数是 64。假设 $I_L = 0.1$, 且 $I_H = 0.5$, β_l 均为 1。

2.2 HSLACO-OFDM 层间功率比例因子最优化设置方法

对于 HSLACO-OFDM 信号, 在第 l 层中仅调制 $N/2^l$ 个子载波, 并在 $m2^l (m = 0, 1, \dots, N/2^l - 1)$ 子载

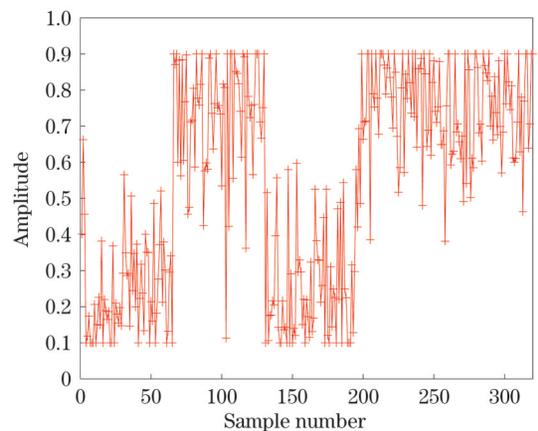


图 5 HSLACO-OFDM 信号波形图

Fig. 5 Waveform of HSLACO-OFDM signal

波上叠加了周期信号 s_n , 根据 Parseval 定理, 未限幅时域信号的方差为 $\sigma^2/2^l$ 。因此各层信号的方差 σ_l 可由

下式给出:

$$\sigma_l = \frac{\sigma}{\beta_l 2^{\frac{l}{2}}} \quad (19)$$

在频域中,第 l 层的电功率为 σ_l^2 ,假设来自所有层的频域电功率之和为 ζ 。根据式(19), ζ 可以表示为

$$\sum_{l=1}^L \frac{1}{2^l} \frac{\sigma^2}{\beta_l^2} + \sigma_{s_n}^2 = \zeta \quad (20)$$

通常将光无线信道建模为具有加性高斯白噪声(AWGN)的线性时不变信道。在实际场景中,限幅概率可能很小。在 AWGN 信道下,忽略限幅效应时,HSLACO-OFDM 可实现速率可以用下式来估计^[24]:

$$C = \sum_{l=1}^L \frac{W}{2^{l+1}} \log_2(1 + R_{\text{SNR}l}) =$$

$$\sum_{l=1}^L \frac{W}{2^{l+1}} \log_2 \left(1 + \frac{\sigma^2 [H(f)]^2 + \sigma_{s_n}^2}{\alpha \beta_l^2 \sigma_N^2} \right), \quad (21)$$

式中: $R_{\text{SNR}l}$ 表示第 l 层信号的信噪比; $H(f)$ 表示频域中的信道频率响应; σ_N^2 表示噪声功率; W 表示整个带宽。 $H(f)$ 在有效频带内可以认为是常数,在推导过程中可设置1。

一般系统中,认为电功率值是有限的,因此在电功率 ζ 为固定值的约束下,以实现最高通信速率为目标,将式(21)和式(20)联立为拉格朗日函数:

$$\mathcal{L}(\beta_1, \dots, \beta_L, \lambda) = \sum_{l=1}^L \frac{W}{2^{l+1}} \log_2 \left(1 + \frac{\sigma^2 + \sigma_{s_n}^2}{\alpha \beta_l^2 \sigma_N^2} \right) - \lambda \cdot \left(\sum_{l=1}^L \frac{1}{2^l} \frac{\sigma^2}{\beta_l^2} - \zeta \right) \quad (22)$$

其偏导数计算如下:

$$\frac{\partial \mathcal{L}(\beta_1, \dots, \beta_L, \lambda)}{\partial \beta_l} = \frac{W}{2^{l+1} \ln 2} \frac{-2(\sigma^2 + \sigma_{s_n}^2)}{\alpha \sigma_N^2 \beta_l^3} - \lambda \frac{1}{2^l} \frac{-2\sigma^2}{\beta_l^3} + \lambda \sigma_{s_n}^2 \quad (23)$$

通过将偏导数设定为0,可以获得最优光功率分配为

$$\beta_l = \sqrt{\frac{2\lambda(\sigma^2 + \sigma_{s_n}^2) \ln 2}{W - 2\lambda\alpha\sigma_N^2 \ln 2} - \lambda\sigma_{s_n}^2} \quad (24)$$

拉格朗日乘数 λ 可以根据式(24)和式(20)来计算,其值为

$$\lambda = \frac{1}{2 \ln 2} \frac{(2^L - 1)W}{2^L \zeta + (2^L - 1)\alpha\sigma_N^2 + \sigma_{s_n}^2} \quad (25)$$

在不同层的信号中,参数 λ , W , σ , $\sigma_{s_n}^2$ 和 σ_N 相同,因

此每层的最优比例应该是相同的,此时,信号传输速率达到最大值。

2.3 调光约束下 HSLACO-OFDM 混合比例因子确定方法

根据 HSLACO-OFDM 的混合原理,通过调整 α 和 β_l 来实现所需的调光级别。但是,其混合比例因子需满足限幅比约束、误码率性能约束等,同时应满足上节分析的最高速率分配原则。因此约束可以表示为^[14, 22]

$$\left\{ \begin{array}{l} P(I_Y > I_H) = P(I_Z < I_L) \leq \gamma \\ P_b = \frac{\sum_{l=1}^L \frac{1}{2^{l+1}} \log_2 M_l \times \frac{4(\sqrt{M_l} - 1)}{\sqrt{M_l} \log_2 M_l} Q\left(\sqrt{\frac{3}{M_l - 1} \frac{\sigma^2}{4N_0 \beta_l^2}}\right)}{\sum_{l=1}^L \frac{1}{2^{l+1}} \log_2 M_l} \leq \epsilon, \\ \beta_1 = \beta_2 = \dots = \beta_L = \beta \end{array} \right. \quad (26)$$

式中: γ 表示限幅比约束; ϵ 表示目标误码率; M_l 是第 l 层的 QAM 的星座阶数。

需要注意的是叠加的 s_n 信号并不改变符号的最大值,且在解调时会被去掉,因此对限幅比和误码率均没有影响。

调光因子有 α 和 β 两个自由度,如果两者都改变则较难分析。可以注意到,当 $\alpha = 0$ 时,HSLACO-OFDM 信号中完全传输 SLACO-OFDM 信号,可以通

过调整 β 实现低亮度等级调整。同理,当 $\alpha = 1$ 时,HSLACO-OFDM 信号中完全传输 NSLACO-OFDM 信号,可以通过调整 β 实现高亮度等级调整。对于中等亮度等级,应当混合传输 SLACO-OFDM 和 NSLACO-OFDM 信号,可通过固定 β 、改变 α 来实现调光等级目标。

根据上述原则,假设目标调光等级为 η_p 。根据式(15)和式(18),可以得到 α 和 β 的取值如表 1 所示。

表 1 不同调光等级区间的比例因子取值

Table 1 Scaling factor values for different dimming level intervals

Value interval of η_p	α	β
$0 \leq \eta_p < \eta_{low}$	0	$\frac{\sum_{i=1}^L \frac{\sigma}{\sqrt{2\pi} 2^{i/2}}}{\eta(I_H - I_L) - \sigma_{s_n}}$
$\eta_{low} \leq \eta_p \leq \eta_{high}$	$\frac{\eta_p(I_H - I_L) - \sum_{i=1}^L \frac{\sigma}{\beta_0 \sqrt{2\pi} 2^{i/2}} - \sigma_{s_n}}{I_H - I_L - 2 \sum_{i=1}^L \frac{\sigma}{\beta_0 \sqrt{2\pi} 2^{i/2}} - 2\sigma_{s_n}}$	β_0
$\eta_{high} < \eta_p \leq 1$	1	$\frac{\sum_{i=1}^L \frac{\sigma}{\sqrt{2\pi} 2^{i/2}}}{(1 - \eta)(I_H - I_L) + \sigma_{s_n}}$

表 1 中:

$$\left\{ \begin{aligned} \eta_{low} &= \frac{\sum_{i=1}^L \frac{\sigma}{\sqrt{2\pi} 2^{i/2}} + \sigma_{s_n}}{I_H - I_L} \\ \eta_{high} &= 1 - \frac{\sum_{i=1}^L \frac{\sigma}{\sqrt{2\pi} 2^{i/2}} + \sigma_{s_n}}{I_H - I_L} \end{aligned} \right. ; \quad (27)$$

β_0 为满足约束条件式(26)的 β 的最小值,其值可根据数值仿真确定。

3 仿真结果分析

通过仿真评估所提出的 HSLACO-OFDM 的性能。在本节的仿真中,LED 动态范围经过归一化后,设置为 $[0, 1]$ 。

图 6 比较了 4 层 HSLACO-OFDM 和 LACO-OFDM 采用 16QAM、32QAM 和 64QAM 调制方式时的误码率性能。仿真中,噪声功率设置为 -5 dBm (例如噪声功率密度为 -95 dBm/Hz,信号带宽为 100 MHz),平均振幅调整为 0.5。对于 HSLACO-OFDM, α 的值为 0.5,信号的直流幅度根据动态范围进行自适应的调整。

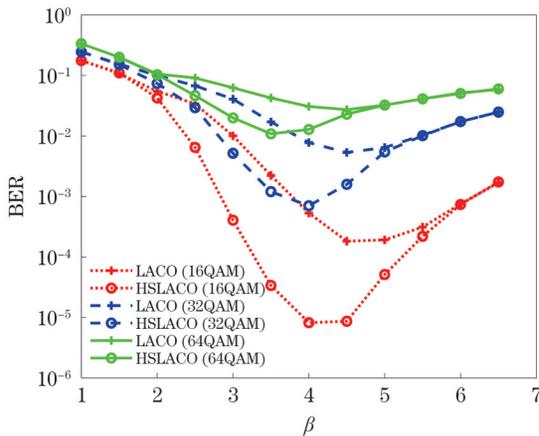


图 6 HSLACO-OFDM 与 LACO-OFDM 的误码率性能比较
Fig. 6 Comparison of BER performance between HSLACO-OFDM and LACO-OFDM

从图 6 可以看出,在相同的 QAM 调制阶数条件下,当 β 从 1 到 6.5 变化时,误码率先减小后增大。主要原因是随着 β 的增大,信号的限幅噪声减少,误码率改善。但是 β 过大也会导致信号功率变小,进而导致误码率性能恶化。而 β_0 可取 BER 最小时对应的 β 值。从结果中可以看出,与 LACO-OFDM 相比,在仿真参数相同的情况下,所提出的 HSLACO-OFDM 信号具有更好的误码率性能。

在考虑调光约束的条件下,对 HSLACO-OFDM 的频谱效率进行仿真,结果如图 7 和图 8 所示,其中噪声功率分别为 -15 dBm 和 -5 dBm (例如噪声功率密度为 -95 dBm/Hz,信号带宽分别为 100 MHz 和 1 GHz)。图中还给出了 DCO-OFDM 和 4 层 ABLO-OFDM、RLACO-OFDM 的性能,以供比较。

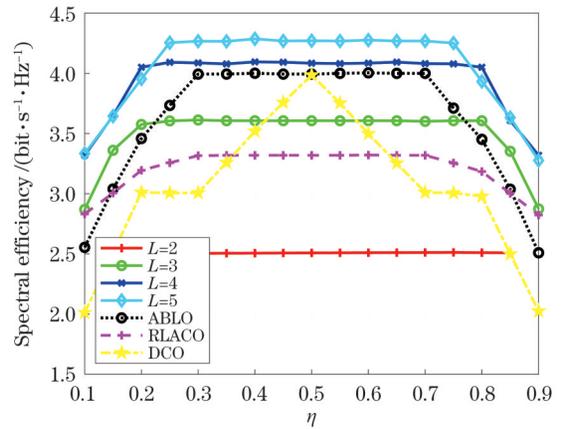


图 7 HSLACO-OFDM 与 ABLO-OFDM、RLACO-OFDM 和 DCO-OFDM 的频谱效率性能比较,噪声功率 -15 dBm
Fig. 7 Comparison of spectral efficiency among HSLACO-OFDM, ABLO-OFDM, RLACO-OFDM, and DCO-OFDM when noise power is set to -15 dBm

可以看出,DCO-OFDM 由于没有利用多层叠加,虽然实现上复杂度最低,但是频谱效率较差。在层数相同的情况下,对于中间调光级别,所提出的方案可以实现比传统的 RLACO-OFDM、ABLO-OFDM 更高的频谱效率。与 4 层 ABO-OFDM 相比,4 层

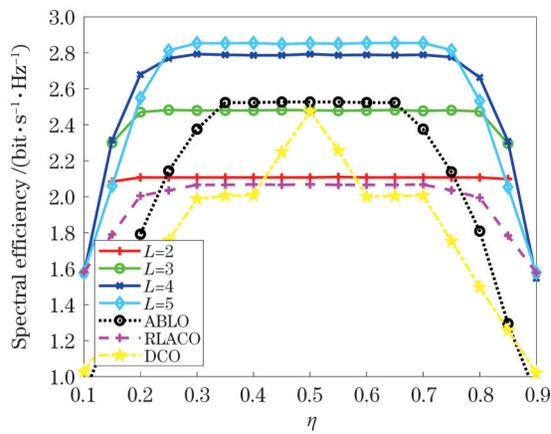


图8 HSLACO-OFDM与ABLO-OFDM、RLACO-OFDM和DCO-OFDM的频谱效率性能比较,噪声功率 -5 dBm
Fig. 8 Comparison of spectral efficiency among HSLACO-OFDM, ABLO-OFDM, RLACO-OFDM, and DCO-OFDM when noise power is set to -5 dBm

HSLACO-OFDM的频谱效率提高了约 0.2 (bit/s)/Hz。从仿真结果可以看出,在相同层数和噪声环境的条件下,HSLACO-OFDM的频谱效率相对于其他调制方式更高,因为它占用更多的子载波且具有更低的峰均功率比。在计算复杂度方面,当层数相同时,HSLACO-OFDM和RLACO-OFDM、ABLO-OFDM相比主要是增加了分组求最大值运算、信号叠加、直流调整等简单计算过程,计算复杂度基本持平。从结构复杂度来说,HSLACO-OFDM发射部分增加了负向信号支路,需要两个周期信号生成叠加支路,较单支路的RLACO-OFDM、ABLO-OFDM略有增加。三种方法均与LACO-OFDM接收机兼容,因此接收复杂度相同。

从仿真结果可以总结出,对于HSLACO-OFDM,最佳叠加层数随噪声功率和调光等级的变化而变化。对比图7和图8可知:对于低亮度和高亮度情况,5层的频谱效率低于4层;对于中等亮度的调光等级,5层的频谱效率较高。但是在高噪声环境下,5层的频谱效率提升不大,且复杂度较高,因此在低亮度和高亮度或高噪声环境下,应采用较低的叠加层数。在中等调光级别和低噪声环境中工作,可以采用更多叠加层数的方案。

4 结 论

为了实现可见光通信的调光控制,本文基于SLACO-OFDM低峰均功率比多层叠加调制方式,通过将SLACO-OFDM和NSLACO-OFDM信号相结合,设计了HSLACO-OFDM调光调制方式。给出了在最小误码率和调光约束条件下的混合比例计算方法。提出的HSLACO-OFDM充分利用了LED整个动态范围,其混合信号比例可调,可以达到所需的亮度。由于HSLACO-OFDM具有更低的峰均功率比,

因此可以在较宽的光照亮度调节范围内获得相对稳定的传输效率。仿真结果表明,该方案在误码率性能和频谱利用率上比其他常用多层调制和调光OFDM方案更有优势。

参 考 文 献

- [1] Haas H, Yin L, Chen C, et al. Introduction to indoor networking concepts and challenges in LiFi[J]. Journal of Optical Communications and Networking, 2019, 12(2): A190-A203.
- [2] Kumar S, Singh P. A comprehensive survey of visible light communication: potential and challenges[J]. Wireless Personal Communications, 2019, 109(2): 1357-1375.
- [3] Nguyen T, Islim M S, Chen C, et al. iDim: practical implementation of index modulation for LiFi dimming[J]. IEEE Transactions on Green Communications and Networking, 2021, 5(4): 1880-1891.
- [4] 李琳,王超,郭家宁,等.基于删除Polar码的可调光可见光通信方案[J].光学学报,2022,42(16):1606007.
Li L, Wang C, Guo J N, et al. Dimmable visible light communication scheme based on deleting polar code[J]. Acta Optica Sinica, 2022, 42(16): 1606007.
- [5] Hei Y Q, Kou Y C, Shi G M, et al. Energy-spectral efficiency tradeoff in DCO-OFDM visible light communication system[J]. IEEE Transactions on Vehicular Technology, 2019, 68(10): 9872-9882.
- [6] Mohammed M M A, He C W, Armstrong J. Diversity combining in layered asymmetrically clipped optical OFDM[J]. Journal of Lightwave Technology, 2017, 35(11): 2078-2085.
- [7] Huang X, Yang F, Pan C Y, et al. Advanced ADO-OFDM with adaptive subcarrier assignment and optimized power allocation[J]. IEEE Wireless Communications Letters, 2019, 8(4): 1167-1170.
- [8] Huang X, Yang F, Liu X, et al. Subcarrier and power allocations for dimmable enhanced ADO-OFDM with iterative interference cancellation[J]. IEEE Access, 2019, 7: 28422-28435.
- [9] Wang T, Hou Y H, Zhang H Y. The spectral efficiency augmented HACO-OFDM based visible light communications[J]. Optics Communications, 2019, 437: 178-183.
- [10] Wang Q, Wang Z C, Dai L L. Asymmetrical hybrid optical OFDM for visible light communications with dimming control[J]. IEEE Photonics Technology Letters, 2015, 27(9): 974-977.
- [11] 贾科军,靳斌,郝莉,等.室内可见光通信中DCO-OFDM和ACO-OFDM系统性能分析[J].中国激光,2017,44(8):0806003.
Jia K J, Jin B, Hao L, et al. Performance analysis of DCO-OFDM and ACO-OFDM systems in indoor visible light communications [J]. Chinese Journal of Lasers, 2017, 44(8): 0806003.
- [12] Islam R, Mondal M R H. Hybrid DCO-OFDM, ACO-OFDM and PAM-DMT for dimmable LiFi[J]. Optik, 2019, 180: 939-952.
- [13] Li B L, Xu W, Feng S M, et al. Spectral-efficient reconstructed LACO-OFDM transmission for dimming compatible visible light communications[J]. IEEE Photonics Journal, 2019, 11(1): 7900714.
- [14] Zhang X Y, Wang Q, Zhang R, et al. Performance analysis of layered ACO-OFDM[J]. IEEE Access, 2017, 5: 18366-18381.
- [15] Li B L, Xue X M, Feng S M, et al. Layered optical OFDM with adaptive bias for dimming compatible visible light communications [J]. Journal of Lightwave Technology, 2021, 39(11): 3434-3444.
- [16] Zhang T, Zou Y, Sun J N, et al. Improved companding transform for PAPR reduction in ACO-OFDM-based VLC systems[J]. IEEE Communications Letters, 2018, 22(6): 1180-1183.
- [17] 徐宪莹,岳殿武.基于复星座映射哈特莱变换的新型光空间调制正交频分复用[J].中国激光,2021,48(9):0906002.
Xu X Y, Yue D W. A novel optical spatial modulation OFDM based on complex constellation mapping with Hartley transform[J]. Chinese Journal of Lasers, 2021, 48(9): 0906002.
- [18] Hu W W. PAPR reduction in DCO-OFDM visible light

- communication systems using optimized odd and even sequences combination[J]. IEEE Photonics Journal, 2019, 11(1): 7901115.
- [19] 刘晓爽, 李建锋, 任亚浩, 等. 无线光通信中 LACO-OFDM 的非迭代检测接收方法[J]. 中国激光, 2022, 49(11): 1106002.
- Liu X S, Li J F, Ren Y H, et al. Non-iterative detection receiving method of LACO-OFDM in wireless optical communication[J]. Chinese Journal of Lasers, 2022, 49(11): 1106002.
- [20] Feng S M, Feng H L, Zhou Y, et al. Low-complexity hybrid optical OFDM with high spectrum efficiency for dimming compatible VLC system[J]. Applied Sciences, 2019, 9(18): 3666.
- [21] Li B L, Feng S M, Xu W, et al. Interference-free hybrid optical OFDM with low-complexity receiver for wireless optical communications[J]. IEEE Communications Letters, 2019, 23(5): 818-821.
- [22] Sun Y Q, Yang F, Gao J N. Novel dimmable visible light communication approach based on hybrid LACO-OFDM[J]. Journal of Lightwave Technology, 2018, 36(20): 4942-4951.
- [23] Dissanayake S D, Armstrong J. Comparison of ACO-OFDM, DCO-OFDM and ADO-OFDM in IM/DD systems[J]. Journal of Lightwave Technology, 2013, 31(7): 1063-1072.
- [24] Li X, Mardling R, Armstrong J. Channel capacity of IM/DD optical communication systems and of ACO-OFDM[C] // 2007 IEEE International Conference on Communications, June 24-28, 2007, Glasgow, UK. New York: IEEE Press, 2007: 2128-2133.

Dimming Controllable Hybrid Multilayer OFDM Modulation Method for Indoor Visible Light Communication

Ren Jiawei, Wang Tao, Xu Zhijian, Qu Jing*

School of Information System Engineering, Information Engineering University, Zhengzhou 450001, Henan, China

Abstract

Objective Indoor visible light communication systems generally need to provide both communication and lighting services, and in order to meet the standard requirements for indoor lighting, indoor visible light communication systems must have brightness control (also called dimming control). Therefore, it is imperative to design indoor visible light signal modulation methods that can perform dimming control. Indoor high-speed visible light communication often uses orthogonal frequency division multiplexing (OFDM) modulation to achieve high-speed transmission, and traditional optical OFDM research mainly focuses on improving data transmission rate, which cannot effectively support dimming control, resulting in poor user experience. Therefore, dimmable OFDM modulation schemes adapted to communication-lighting integrated applications need to be designed. In OFDM dimming design, a balance between transmission efficiency and dimming capability is required. Direct current biased optical OFDM (DCO-OFDM) controls the brightness level directly by controlling the DC bias level, but it may limit and thus corrupt the signal waveform. By superimposing layered asymmetrically clipped optical OFDM (LACO-OFDM) with multiple positives and negatives, it achieves both dimming and improved spectral efficiency by using the multi-layer transmission. However, the multi-layer superposition characteristic of LACO-OFDM leads to a relatively high peak-to-average-power ratio and deteriorating the bit error rate (BER) performance at specific dimming levels.

Methods For the lighting demand and dimming requirement of visible light communication, this paper proposes a hybrid superimposed LACO-OFDM (HSLACO-OFDM) modulation method based on LACO-OFDM modulation. According to the principle of LACO-OFDM signal formation and subcarrier occupancy in each layer, it can be seen that after the superposition of signals in the L th layer, there will still be some subcarriers that are not used. The superposition of the adjusted signals on these subcarriers does not interfere with the signals of the LACO-OFDM layers. Therefore, we can design a time domain amplitude adjustment of the LACO-OFDM signal after superimposing the signals using these subcarriers to generate the superimposed LACO-OFDM (SLACO-OFDM) signal. For SLACO-OFDM signals, the receiver can detect the signal layer by layer using the same method of successive interference cancellation as for LACO-OFDM signal detection. By combining SLACO-OFDM and its negative signal NSLACO-OFDM through time division multiplexing, the HSLACO-OFDM signal is formed. The proposed HSLACO-OFDM makes full use of the entire dynamic range of light emitting diodes (LEDs) with adjustable mixed signal ratios to achieve the desired brightness. We propose an optimal setting of the HSLACO-OFDM interlayer power scaling factor using a Lagrangian function under a certain constraint of electrical power. It is also proved that the optimal ratio should be the same in each layer because the parameters are the same in different layers, when the signal transmission rate reaches the maximum. We also investigate the HSLACO-OFDM hybrid scaling factor determination method under dimming constraints. The two degrees of freedom of the dimming factor are analyzed, and the method of taking values under different dimming levels is given.

Results and Discussions Simulations are performed to evaluate the performance of the proposed HSLACO-OFDM. It is also compared with DCO-OFDM, reconstructed LACO-OFDM (RLACO-OFDM), and adaptively biased layered optical OFDM (ABLO-OFDM). The BER performances of 4-layer HSLACO-OFDM and LACO-OFDM with 16-ary quadrature amplitude modulation (QAM), 32-ary QAM (32QAM) and 64-ary QAM (64QAM) modulation are simulated (Fig. 6). At the same QAM modulation order, the BER decreases and then increases as the dimming factor changes from 1 to 6.5. The main reason is that as the dimming factor increases, the limiting noise of the signal decreases and the BER improves. However, too large dimming factor can also lead to a

smaller signal power, resulting in a deterioration of the BER performance. And the dimming factor can be taken as the value corresponding to the smallest BER. From the results, it can be seen that the proposed HSLACO-OFDM signal has better BER performance compared with LACO-OFDM under the same simulation parameters. The spectral efficiency of HSLACO-OFDM under the condition of dimming constraint is simulated (Figs. 7 and 8). For the same number of layers, the proposed scheme can achieve higher spectral efficiency than the conventional RLACO-OFDM and ABLO-OFDM for intermediate dimming levels. From the simulation results, it can be summarized that for HSLACO-OFDM, the optimal number of stacked layers varies with the noise power and dimming level. In low brightness and high brightness or high noise environments, a lower number of stacked layers should be used. When working in medium dimming level and low noise environment, more stacked layers can be used.

Conclusions In order to realize the dimming control of visible light communication, this paper designs the HSLACO-OFDM dimming modulation based on SLACO-OFDM low peak-to-average-power ratio multilayer superposition modulation by combining SLACO-OFDM and NSLACO-OFDM signals. The hybrid ratio calculation method under the minimum BER and dimming constraints is given. The proposed HSLACO-OFDM makes full use of the entire dynamic range of LEDs with adjustable mixing signal ratio to achieve the desired brightness. Since HSLACO-OFDM has a lower peak-to-average-power ratio, a relatively stable transmission efficiency can be obtained over a wide adjustable range of light brightness. Simulation results show that this scheme has advantages over other commonly used multilayer modulation and dimming OFDM schemes in terms of BER performance and spectrum utilization.

Key words optical communications; visible light communication (VLC); dimming control; peak-to-average-power ratio; hybrid multilayer modulation